CrossMark

Physically-Based and Power-Law Constitutive Relations for Higher Temperature Metal Processing and Creep-Type Deformations

R.W. ARMSTRONG[1,3] and N. BALASUBRAMANIAN[2]

1.—Department of Mechanical Engineering, University of Maryland, College Park, MD 20742, USA. 2.—VLN Prabuddhalaya, Bannerghatta P.O., Bangalore 560083, India. 3.—e-mail: rona@umd.edu

There is continuing research interest in the development and use of constitutive relations for assistance with description and optimization of higher temperature metal and alloy processing conditions and desired mechanical property performances, particularly in the latter case for nanopolycrystalline materials under creep-type loading deformations. Here, we focus on the plastic flow stress dependence on strain rate, temperature, and especially, on material grain size. Connection is established between, on the one hand, relatively recent thermal-activation-based relations for dislocation motion and, on the other hand, comparative power law expressions.

INTRODUCTION

A brief description is given of thermally-activated dislocation relations and power law descriptions. The thermal activation description will be seen to follow-on from the article in *JOM* by Conrad on "Thermally Activated Deformation of Metals", published slightly more than 50 years ago and continuing to be an important reference on the topic.[1]

Thermal Activation-Strain Rate Analysis (TASRA) Description

Conrad's description had followed-on in turn from the pioneering analysis of temperature and strain rate influences on single crystal deformation behaviors by Seeger in which a thermal component of shear stress, τ_{Th}, is taken to control the temperature and strain rate dependencies of plastic flow by means of dislocation motion.[2] The model presumes that τ_{Th}, as one component of the total shear stress, is a function only of the strain rate, $d\Upsilon/dt$, and absolute temperature, T. Very importantly, the assumption leads to a restrictive mathematical condition, then between the three mechanical test conditions of: (1) the dependence of the natural logarithm of shear strain rate, $\ln(d\Upsilon/dt)$, on τ_{Th} at constant temperature, T; (2) the dependence of τ_{Th} on T at constant $(d\Upsilon/dt)$; and (3) the reciprocal dependence of $(d\Upsilon/dt)$ on T at constant τ_{Th}:

$$[\partial \ln(d\Upsilon/dt)/\partial\tau_{\mathrm{Th}}]_{\mathrm{T}}[\partial\tau_{\mathrm{Th}}/\partial T]_{\ln(d\Upsilon/dt)}[\partial T/\partial \ln(d\Upsilon/dt)]_{\tau\mathrm{Th}}= -1.0$$

$$(1)$$

The first factor in Eq. 1 is a measure of the material strain rate sensitivity and leads to a definition of the thermal activation area, A^*, or dimensionally, an activation "volume", $v^* = A^*b$, in which b is the dislocation Burgers vector in the plane of A^*. The quantity v^* is often employed to characterize the material rate dependence according to:

$$v^* = A^*b = kT[\partial \ln(d\Upsilon/dt)/\partial\tau_{\mathrm{Th}}]_{\mathrm{T}} \qquad (2)$$

In Eq. 2, k is Boltzmann's constant. The second factor in Eq. 1, for temperature dependence, applies for normal thermal softening, an exception to which will be mentioned later for an initial condition in the observation of serrated plastic flow. And the third factor is taken to apply, for example, in the establishment of a steady-state creep rate at constant tensile or compressive flow stress, σ, as historically described, for example, by Orowan.[3]

Armstrong gave an early TASRA account of the application of Eq. 1 to polycrystalline deformation behavior for which the component shear stress, τ_{Th}, was related to the flow stress, σ_ε, at true strain, ε, in an expanded description of the Hall–Petch (H–P) relationship as:[4]

Physically-Based and Power-Law Constitutive Relations for Higher Temperature Metal Processing and Creep-Type Deformations

823

$$\tau_{\text{Th}} = (1/m_{\text{T}})\left[\sigma_\varepsilon - \sigma_{G\varepsilon} - k_\varepsilon \ell^{-1/2}\right] \qquad (3)$$

In Eq. 3, m_{T} is a Taylor orientation factor that also relates to the shear strain rate connection with unidirectional strain, ε, as $(d\Upsilon/dt) = m_{\text{T}}(d\varepsilon/dt)$; $\sigma_{G\varepsilon}$ is an athermal stress component that is dependent on solute content, dislocation density and elastic shear modulus; k_ε is a microstructural stress intensity (H–P slope); and ℓ is the average grain diameter, generally specified on a linear intercept basis. Equation 3 is well-established at lower temperatures and higher strain rates,[5] but the interest here is to connect with current applications being made to higher temperature measurements, especially at finer grain sizes.

Thermal activation enters explicitly into the TASRA description through the rate equation:

$$(d\Upsilon/dt) = (d\Upsilon/dt)_0 \exp(-G\{\tau_{\text{Th}}\}/kT) \qquad (4)$$

In Eq. 4, $(d\Upsilon/dt)_0$ is a reference plastic shear strain rate and $G\{\tau_{\text{Th}}\}$ is a reference Gibbs free energy taken to depend only on τ_{Th}; that is: $G\{\tau_{\text{Th}}\} = G_0 - \int v^* d\tau_{\text{Th}}$. Li, among others, had pointed out experimentally that an inverse dependence of A^* (or v^*) on τ_{Th} should lead to a power law dependence of dislocation velocity on τ_{Th}.[6] Recently, such $v^* = W_0/\tau_{\text{Th}}$ dependence has been established for a compilation of measurements covering a range between the lowest strain rate creep deformation results to the highest rate shock loading conditions, as shown in Fig. 1.[7] The broad coverage of measurements depicted in the figure,[8] which includes the most recently added 'dotted-line' dependencies for high-temperature creep measurements among many others reported by Balasubramanian and Li for ferritic and austenitic steel materials,[9] encourages connection of the TASRA description with other higher temperature rate dependencies.

The indicated $v^* - \tau_{\text{Th}}$ dependence had been employed in the development of the so-called Zerilli–Armstrong (Z–A) relations which were applied to lower temperature/higher rate material dynamics calculations based on the expression:[10,11]

$$(d\Upsilon/dt) = (d\Upsilon/dt)_0 [\exp(-G_0/kT)](\tau_{\text{Th}}/\tau_{\text{Th0}})^{Wo/kT} \qquad (5)$$

In Eq. 5, τ_{Th0} is a lower limiting reference shear stress. More recently, Eq. 5 has been employed in a number of higher temperature applications, as will be described in the following report. At higher temperatures, there is also evidence for the H–P k_ε in Eq. 3 becoming vanishingly small or even negative,[12] as will also be discussed in relation to grain boundary weakening.

Power Law (P-L) Description

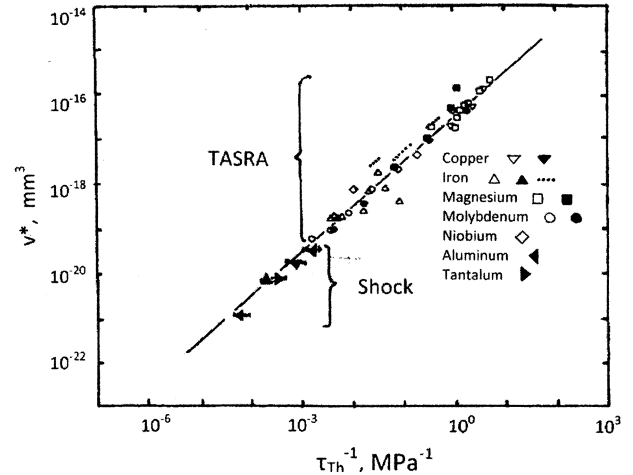We begin with the pioneering Zener–Hollomon (Z–H) relation:[13]

Fig. 1. TASRA activation "volume", v^* $(=A^* b)$, dependence on thermal component of shear stress, τ_{Th}, for creep, conventional σ–ε, and shock measurements[8].

$$(Z - H)_0 = (d\varepsilon/dt)_0 = \text{constant} = (d\varepsilon/dt)\exp(G_0/kT). \qquad (6)$$

Equation 6, for the temperature-compensated plastic strain rate dependence, was initially proposed by Zener and Hollomon to follow a P-L dependence. Figure 2 shows the analogous relation of Z–A and $(Z–H)_0$ descriptions for a number of lower T, higher $(d\varepsilon/dt)$ measurements compiled for α-Ti materials.[7,14] Note might be taken at the lower stress level of the abscissa scale of the figure of a neglected low-stress "bump" in the experimental measurements caused by the occurrence of strain aging behavior leading to serrated flow (to be related to the evaluation of Eq. 1).

Weertman has provided an important review of his own pioneering researches on the development of dislocation model descriptions for the otherwise empirical P-L relation.[15] On the basis of the Orowan relation $(d\Upsilon/dt) = \rho b v$, a σ^3 dependence of $(d\Upsilon/dt)$ was described, first, on the basis of the dislocation density, ρ, being proportional to σ^2 and, second, for a dislocation velocity, v, taken as proportional to σ. Higher exponents are generally measured today. An exponential factor with activation energy, Q, was considered separately to apply for dislocation climb or other diffusion mechanism. Also, the dislocation velocity is known to vary non-linearly with σ at constant ρ. Such considerations of dislocation velocity, activation energy and stress exponents can be compared with the TASRA Eq. 5 description in which the same model parameters occur, for example: $(d\Upsilon/dt)_0 = \rho b v_0$; G_0 applies for the non-linear, thermally-activated, dislocation motion; and an explicit stress exponent obtains from the $v^* - \tau_{\text{Th}}$ relationship.
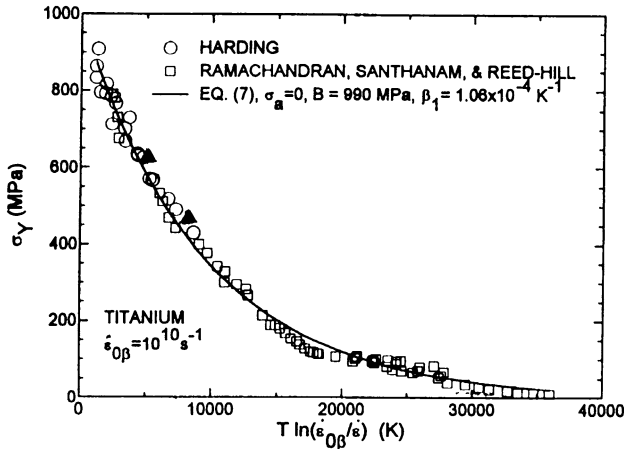
Fig. 2. The yield stress of α-Ti materials accounted for by Z–A description[10] in a temperature-compensated strain rate dependence following the method of Zener and Hollomon.[13] The figure is updated from that presented in Ref. 14 by addition of the *solid-triangle points* added for high rate tensile split-Hopkinson pressure bar measurements of W. Mocko, L. Kruszka and A. Brodecki, in *11th International Conference on the Mechanical and Physical Behavior of Materials under Dynamic Loading, DYMAT 2015, EPJ Web of Conferences*, ed. E. Cadoni, H. Couque and S. Hiermaier, 94, 01011 (2015).

An example modern dislocation description of creep deformation for so-called Harper–Dorn creep has been given by Przystupa and Ardell,[16] following on from their earlier work.[17] In Ref. 16, the dislocation kinetics are described in terms of the growth of individual dislocation links in an evolutionary dislocation network. Thus, the dislocation density within the grain volumes is a controlling factor. Both primary and steady-state creep are considered as compared with only steady-state creep being considered in the present report. As with the Weertman description, there is no grain size effect but the introduction of the dislocation network structure provides for a power factor greater than σ^3. Based on Nabarro's pioneering researches on the topic, Armstrong et al.[18] have established grain size limited regions of operation for Harper–Dorn, Nabarro–Herring and other detailed dislocation mechanisms.

Langdon has incorporated into a P-L relation for $(d\varepsilon/dt)$ a normalized dependence on σ and grain size, ℓ, as:[19]

$$(d\varepsilon/dt) = (AD_L Gb/kT)(b/\ell)^p (\sigma/G)^q \qquad (7)$$

In Eq. 7, the coefficient, A, and exponents, p and q, were taken as positive constants; D_L was designated as a lattice-based mass diffusion coefficient of the standard form; and G, here and in following equations containing the factor, (σ/G), is the shear modulus:

$$D_L = D_0 \exp(-Q/kT) \qquad (8)$$

In the case of superplasticity, D_L is replaced by D_{gb} for grain boundary diffusion. Equation 7 gives a reversed grain size dependence compared to the H–P description in Eq. 3.

The higher temperature grain size weakening described by Eq. 7 at constant strain rate can be compared with a positive H–P dependence at lower *intermediate temperatures* for a strain rate controlled by dynamic recovery, $(d\varepsilon/dt)_{hab}$, as proposed for extensive measurements reported for copper by Blum and Zeng in the comparative relation:[20]

$$(d\varepsilon/dt)_{hab} = A(D_b Gb/kT)(\ell/b)^4 f\{\xi\}(\sigma/G)^8 \qquad (9)$$

In Eq. 9, the subscript on the strain rate applies for a quasi-stationary deformation resistance controlled by high angle grain boundaries, D_b is a high angle boundary diffusion coefficient and $f\{\xi\}$ is a factor for the acceleration of dislocation recovery. Notably, Eq. 9 includes an H–P-type dependence that was also employed in a later description by Blum et al.[21] for measurements obtained on ultrafine-grained copper material processed via equal channel angular pressing (ECAP). Follow-up results on effective grain size strengthening and an increase in the ductility of copper were associated with the formation of high angle grain boundaries in ECAPed smaller grain size copper tested at 473 K and 573 K, as reported by Blum et al.[22,23] In an earlier companion article, Schneibel, Heilmaier, Blum, Hasemann and Shanmugasundaram have shown a reversal in the σ dependence on T from grain size strengthening to weakening for the smallest micron-sized PM 2000 superalloy material.[24]

CONNECTIONS

Normally, $[d\tau_{Th}/dT]_{\ln(d\Upsilon/dt)}$ in Eq. 1 is negative for thermal softening behavior; however, a reversal in sign occurs at the initial rise of the temperature peak at which the previously mentioned strain aging and/or solute-effected serrated plastic flow occurs. The positive $(d\sigma/dT)_{\ln(d\Upsilon/dt)}$ leads to the factor $[\partial\ln(d\Upsilon/dt)/\partial\tau_{Th}]_T$ for the strain rate sensitivity necessarily becoming negative, consistent with the prediction from Eq. 1. At the higher T down-side of the stress-dependent peak, the negative strain rate sensitivity reverses itself to being positive as normally associated with the follow-on continuation of thermal softening. Such a complication in the reported measurements of positive and negative strain rate sensitivity measurements for the behavior has been discussed by Antolovich and Armstrong.[25]

Also, Eq. 3 for the H–P grain size dependence of σ_ε has been added-to in special circumstances with another $k_{sb}\ell_s^{-1/2}$ term for the sub-grain size-dependent strengthening of single crystals and certain polycrystalline materials such as niobium.[26] The consideration also relates to the mentioned intermediate temperature measurements made by Blum and Zeng in which an H–P dependence for the steady-state creep resistance of ultrafine grain copper and nano-structured nickel materials has involved an important discrimination made between the strengthening effects of high-angle and low-angle (sub-grain) boundaries.[20] In another

Physically-Based and Power-Law Constitutive Relations for Higher Temperature Metal Processing and Creep-Type Deformations

825

earlier report, Li, Mueller, Höppel, Göken and Blum reported a (v^*/b^2) dependence on (σ/G) in agreement with the dependence shown in Fig. 1.[27]

On another point, comparison of the listed TASRA and P-L relations shows that the P-L exponent, q, is a relatively complicated function of a combination of TASRA parameters in the relation $q = v^*\sigma/m_T kT$. For example, consider the joined triple influences on q of v^* decreasing with increase in the τ_{Th} component of σ at decreasing T. The evaluation of q in terms of TASRA equivalence makes the spread in reported measurements as a function of temperature understandable; see, for example, the representative measurements of q and v^* in Refs. 28 and 29, respectively.

Langdon and co-workers produced an extensive compilation of measurements for Al alloy and Mg alloy materials showing, on a log/log basis, the dependence of $[(d\varepsilon/dt)(kT/D_{gb})(\ell/b)^2]$ plotted against (σ/G) as reproduced in Fig. 3a and b.[30–32] These data connect through the factor $[(d\varepsilon/dt)/D_{gb}]$ with the form of the Zener–Hollomon (Z–H) parameter in Eq. 6 and with the P-L description in Eq. 7. The authors had predicted a slope of 2.0 but the data indicate a somewhat higher value of ~3 in line with Weertman's early model prediction.[15] A main purpose of the work, however, was to show that the stress and grain size dependence of strain rate was the same for conventional and ultrafine grain size materials, including superplastic material behaviors. In such an equation as (7) involving dimensionless quantities, it is desirable to have the numerical value of the constant as low as possible, say ideally 1.0, relating to the value of A in Eq. 7 being ~10. A similar compilation of $[(d\varepsilon/dt)_S kT/DGb]$ measurements was reported by Mukherjee for an extensive number of face-centered cubic metals, relating also to interest in the same nano-scale grain size regime, and displayed also as a function of (σ/G).[33] Padmanabhan, Leuthold, Wilde and Bhattacharya have reported most recently on different model connections with the P-L application to steady-state creep under low σ, high-homologous T conditions.[34] Padmanabhan et al. considered that a single exponent should not be expected because the power exponent would be different for different physical mechanisms controlling plastic flow. The comment relates, for example, to the Harper–Dorn Ref. 16 in which a slope of 1 was employed to gauge the stress dependence. The general model[17] had led to estimation of a slope possibly greater than 3 in the earlier work.

Based on the reciprocal $\tau_{Th} - v^*$ relationship, the TASRA description provides an explicit stress dependence in the Z–H parameter:

$$(Z-H) = (d\varepsilon/dt)_0 = (d\varepsilon/dt)\exp(G_0/kT)[\tau_{Th}/\tau_{Th0}]^{-W_0/kT}$$
$$= (Z-H)_0[\tau_{Th}/\tau_{Th0}]^{-W_0/kT} \qquad (10)$$

On such log/log basis involving $(Z–H)_0$ on the ordinate axis and τ_{Th} on the abscissa scale, Eq. 10 leads to specification of the slope as (W_0/kT), as will be discussed in connection with slope dependencies obtained for corresponding P-L and graphical Larson–Miller (L–M) plots that, in the latter case, take the form in the TASRA description as:[7]

$$\ln\tau_{Th} = -(k/W_0)[T(\ln\Delta t - \{\ln\Delta t_0 + G_0/kT + \ln\tau_{Th0}\})] \qquad (11)$$

In Eq. 11, Δt is the time to rupture while the term in brackets, $\{\ln\Delta t_0 + G_0/kT + \ln\tau_{Th0}\}$, is taken as a relatively constant parameter, C_1, to which the positive contribution of G_0/kT is a minor term compared to the larger negative values of the two other terms. The Z–A description builds onto an early report by Conrad of correlating TASRA prediction and stress–rupture properties of Nimonic 80A and 90 alloys.[35]

Z–A DESCRIPTION

Zerilli and Armstrong developed different physically-based constitutive relations for body-centered cubic (bcc) α-iron as compared with face-centered cubic (fcc) copper.[10] The Z-A relations are in accordance with the main temperature and strain rate dependence being in the yield stress for the bcc case as compared with being in the strain hardening behavior in the fcc case. Kocks and Mecking have given an excellent review of the thermally-activated strain hardening behavior of fcc metals.[36] Among the hexagonal close-packed (hcp) metals, cadmium, zinc, and magnesium follow an fcc-type dependence and titanium, zirconium and hafnium follow a bcc dependence. A summary description was given by Zerilli.[11] For bcc metals, the flow stress, σ_ε, was expressed in relation to Eq. 3 as

$$\sigma_\varepsilon = \sigma_G + B\exp(-\beta T) + K\varepsilon^n + k_\varepsilon\ell^{-1/2} \qquad (12)$$

In Eq. 12, the second term replaces $m\tau_{Th}$ and the next term accounts for essentially isothermal strain hardening in the σ–ε behavior with power law constants, K and n. The strain rate enters through the relation

$$\beta = \beta_0 - \beta_1\ln(d\varepsilon/dt) \qquad (13)$$

In Eq. 13, β_0 and β_1 are experimental constants rooted in the dislocation model description. Equations 12 and 13 were first applied to the prediction of cylinder impact (Taylor type) results reported for Armco iron material, with the added complication for the occurrence of deformation twinning,[11] and were later applied to the detailed description of extensive σ–ε measurements reported over a wide range of temperatures, $22 \le T \le 790$ K, and strain rates $10^{-4} \le (d\varepsilon/dt) \le 2 \times 10^4$ s^{-1}, for tantalum material.[37]
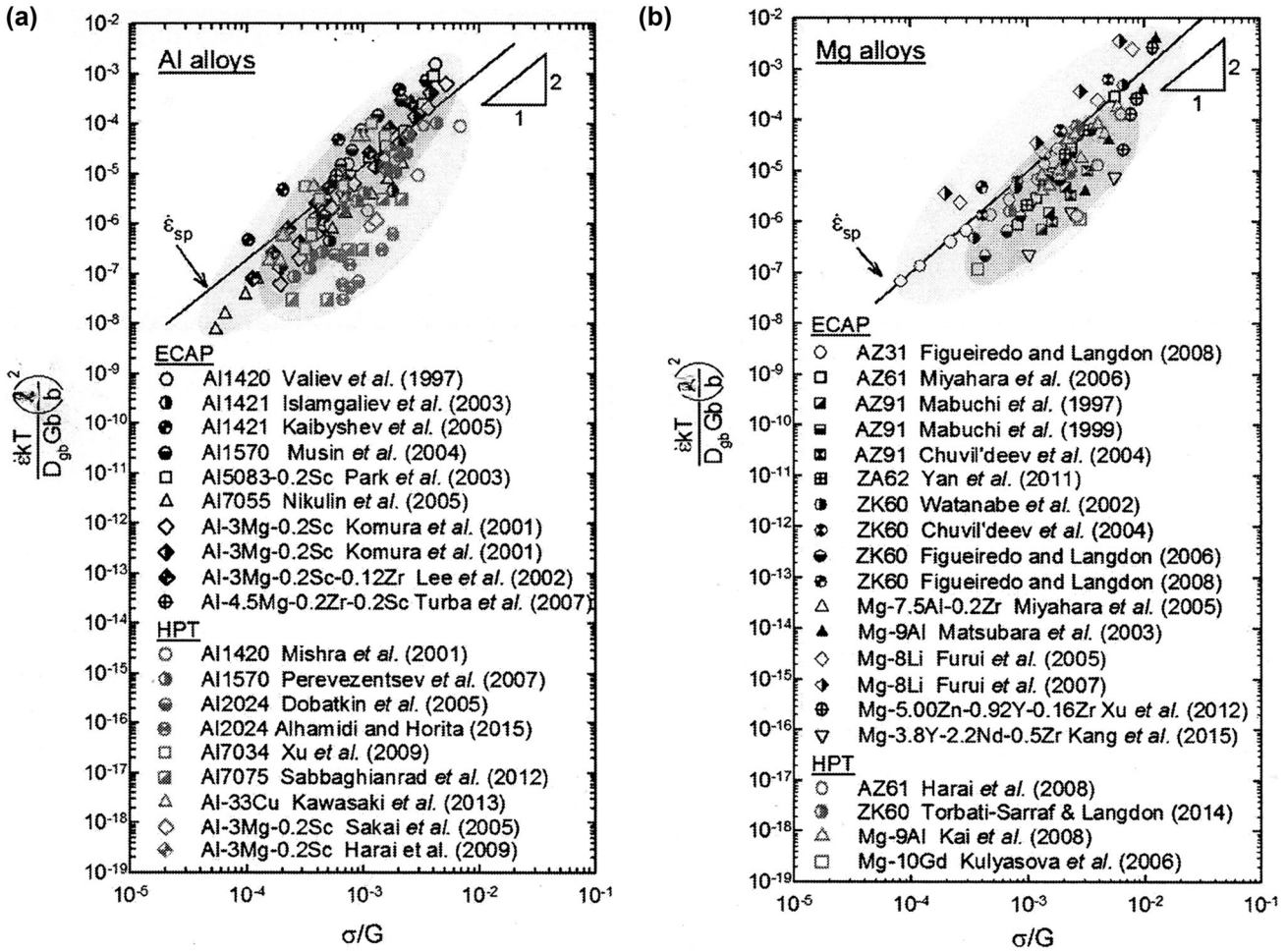
Fig. 3. (a) Compiled measurements for the influence of grain size on superplastic strain rate for Al alloys including materials processed by equal channel angular pressing (*ECAP*) and high pressure torsion (*HTP*) methods. Reprinted from Ref. 30. (b) Compiled measurements for the influence of grain size on superplastic strain rate for Mg alloys including materials processed by *ECAP* and *HPT* methods. Reprinted from Ref. 30.

For thermally-dependent strain hardening in the fcc case, σ_ε, was specified as

$$\sigma_\varepsilon = \sigma_G + B_0 \left[\varepsilon_r \left(1 - e^{-\varepsilon/\varepsilon r} \right) \right]^{1/2} \exp(-\alpha T) + k_\varepsilon \ell^{-1/2} \tag{14}$$

In Eq. 14, the second term involving ε_r accounts for dynamic recovery but otherwise approximates to Taylor-type parabolic strain hardening at smaller strain. The exponential temperature factor, α, follows the same strain rate dependence as β with constants α_1 and α_2. An example comparison both of the calculation with the EPIC-2 code[38] and of the experiment is shown for the impact of a solid copper cylinder in Fig. 4. The dotted and solid profiles are the respective experimental and calculated shapes. The EPIC-2 code calculation provided monitoring of the internal strain contours that are shown. A rise in temperature of ~300 K was monitored at the impact face of the "mushroomed" specimen and might be taken in hindsight as an early indication of the applicability of the Z–A relations for higher

temperature applications. More recent higher temperatures applications have been reported for the plastic flow behavior of β-titanium alloy material by Zhan et al.[39] and for the prediction of hot deformation flow stress results obtained on austenitic steel materials by Mirzaie et al.[40]

SOME APPLICATIONS

Ammouri, Kridli, Ayoub and Hamade have employed Z–A and Z–H descriptions to characterize the deformation behavior of dynamically-recrystallized grain structures achieved in friction stir processing of twin-roll-cast magnesium AZ31 B alloy.[41] A compilation of ambient temperature H–P measurements has been reported for AZ31 materials.[42] Ammouri et al. incorporated the Z–A description within a finite element model. The work followed on from an earlier study by Ammouri and Hamade comparing the performance of Z-A and other constitutive equations among several established relationships,[43] and also followed on from same type grain size measurements made on
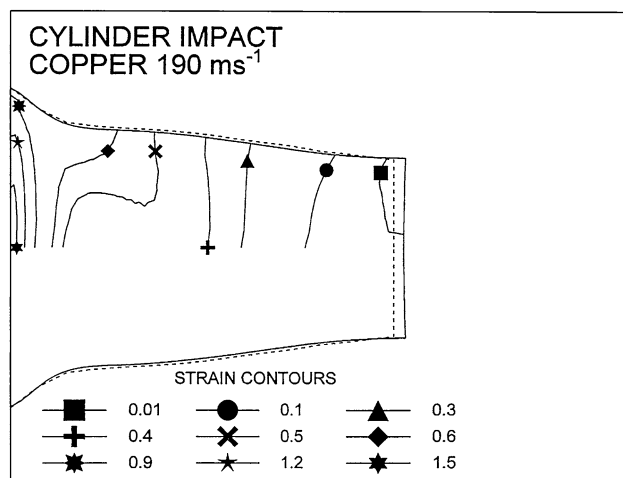
Fig. 4. Comparison of longitudinal center-line section (dotted) experimental and (solid) calculated profiles obtained for a copper cylinder impacted onto a rigid target. Reprinted from Ref. 8.
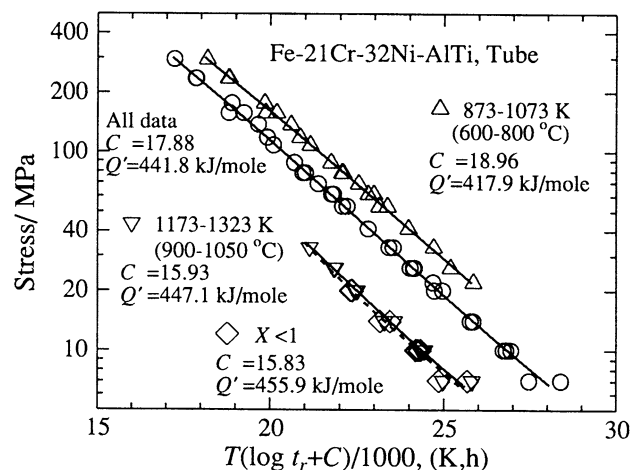

Fig. 5. Larson–Miller plots for compiled creep rupture measurements obtained for designated temperature ranges employed in testing of Fe-21Cr-32Ni-AlTi alloy materials. Reprinted from Ref. 46 by permission kindly provided by M. Tamura.

friction stir-processed AZ31 material, as reported by Chang, Lee and Huang.[44] Both references proposed, with somewhat different numbers, an average experimental relationship between grain size and $(Z–H)_0$ parameter, with significant scatter, of:

$$\ln \ell = 8.81 - 0.24 \ln(Z–H)_0. \quad (15)$$

The comparable Z–A model equation would be:

$$\ln\left(m\tau_{Th0}\Big/\left[\sigma - \sigma_{G\varepsilon} - k\ell^{-1/2}\right]\right) = (kT/W_0)[\ln(Z–H) - \ln(Z–H)_0] \quad (16)$$

In Eq. 16, $\ln(Z–H)$ is the constant $\ln(d\varepsilon/dt)_0$ and strain dependence is indicated in $\sigma_{G\varepsilon}$. On the presumption that the left-side quantities in both equations are proportional, the comparison of the equation right-side slope parameters gives $0.28 < (kT/W_0) < 0.38$ for the Ammouri et al. quoted temperatures of $633 < T < 873$ K. A typical value of $(d\varepsilon/dt)_0 = (d\varepsilon/dt)_{0\beta} = 10^{10}$ s^{-1} might be taken from Fig. 2, and with an average value of $(kT/W_0) = 0.34$ at $T = 753$ K, a value of 7.7 is computed to compare with the 8.81 value given in Eq. 15. The left-side comparison with $\ln\ell$ of Eq. 15, which is equal to $\ln(\tau_{Th0}/\tau_{Th})$, leads to τ_{Th} needing to increase with the decrease in ℓ as $(Z–H)_0$ increases, seemingly consistent with H–P grain size strengthening at higher σ. Were the higher T deformation to involve grain size weakening, the case would be an excellent example of easier higher T material processing, to be then utilized in a lower T grain size strengthened condition.

A second case involves the application to the important consideration of the time to failure, Δt, in shorter term creep testing for the estimation of longer term real service failures. A pioneering

description put forward by Larson and Miller (L–M) for measurements obtained on a number of metals and alloys is still in use:[45]

$$f\{\sigma\} = T[\log \Delta t + 20] \quad (17)$$

In L–M plots, $\log\sigma$ is plotted, after Zener and Hollomon,[13] as $f\{\sigma\}$ on the ordinate scale as a function of the (linear) right-side equation quantity as abscissa. Some variation occurs in the original constant, $C_1 = 20$, while the slope dependence appears to vary within a relatively narrow range, for example, determined to be between -2.0 and -5.5×10^{-4} K^{-1} for the different low-carbon and stainless steel materials investigated by Larson and Miller.[45] Figure 5 shows recently reported comprehensive measurements made by Tamura et al.[46] for 79 types of heat-resistant steels and encompassing the types of steels investigated by Larson and Miller. A slope of -3.4×10^{-4} K^{-1} applies for the 'All data' line in Fig. 5 and compares with $-(k/W_0) = -4.4 \times 10^{-4}$ K^{-1} from Eq. 11. The value of C_1 ranged between ~20 and ~30 for the different materials. The apparent TASRA-based activation energy, Q', was determined as an average value by fitting to the L–M parameter.

More recently, Abe has reported on the several topics of creep, deformation mechanisms and creep lives operative in a well-studied high-temperature (martensitic) Mod.9Cr-1Mo steel material.[47] Abe points importantly to coupled grain growth, ranges in dislocation density (ρ), and variations in precipitate volume fraction and size occurring during creep history, thus establishing that not too much can be expected from application of the more restrictive constitutive equation analyses. Nevertheless, application of the relations given here can be made for a number of the detailed measurements. Abe found that the L–M parameter method led to an over-estimate of creep life and that more

reliable methods are being developed. Logarithmically-plotted minimum creep rates versus $\log\sigma$ gave slope values between 6.0 and 15.0, which values can be compared to a range of $2.4 < (W_0/kT) < 6.0$ determined from Eq. 11, thus showing provision of only part of the explanation for the observed material behavior. The dependence of $\log\sigma$ on Δt gave a slope at 873 K of –0.50 compared to $-(kT/W_0) = -0.39$ and, very importantly, gave agreement with a decreasing slope at higher T.

SUMMARY AND CONCLUSION

1. A number of connections are established between the lower-temperature TASRA-based analysis of dislocation velocity and a higher temperature power law relationship. Diminishing differences seem now to exist between the two descriptions.
2. The review discusses the application of constitutive relations to the deformation of coarse grain, ultrafine-grain and nano-grain materials.
3. The recrystallized grain structure developed in friction stir processing, and whose deformation properties were described using a finite element calculation incorporating the Z-A equations, are shown to exhibit reasonable agreement with grain size prediction obtained on the same TASRA basis.
4. The experimentally-observed grain size dependence of the Zener–Hollomon parameter is rationalized using a Z-A approach.
5. The present review and analysis of higher temperature measurements provide evidence of progress in a challenging regime for design and processing of 'real engineering materials'.

NOTE ADDED IN-PROOF

Recent publication is noted of the relevant article by X. Wang, K. Chandrashekhara, S.A. Rummel, S. Lekakh, D.C. Van Aken and R.J. O'Malley, "Modeling of mass flow behavior of hot rolled low alloy steel based on combined Johnson-Cook and Zerilli-Armstrong model", J. Mater. Sci. 52, 2800 (2017).

REFERENCES

1. H. Conrad, *JOM* 16 (7), 582 (1964).
2. A. Seeger, *Dislocations and the Mechanical Properties of Crystals*, ed. J.C. Fisher, W.G. Johnston, R. Thomson, and T. Vreeland, Jr. (New York, NY: Wiley, 1957), p. 243.
3. E. Orowan, *J. West Scotl. Iron Steel Inst.* 54, 45 (1946).
4. R.W. Armstrong, *J. Sci. Ind. Res.* 32, 591 (1973).
5. R.W. Armstrong, *(Jpn) Mater. Trans.* 55, 2 (2014).
6. J.C.M. Li, *Dislocation Dynamics*, ed. A.R. Rosenfield, G.T. Hahn, A.L. Bement, Jr, and R.I. Jaffee (New York: McGraw-Hill, 1968), p. 87.
7. R.W. Armstrong, in *14th International Conference on Fracture (ICF14), David Taplin Symposium*, ed. A Saxena (Rhodes, GR, 2017).
8. R.W. Armstrong and Q.Z. Li, *Metall. Mater. Trans. A* 46A, 4438 (2015).
9. N. Balasubramanian and J.C.M. Li, *J. Mater. Sci.* 5, 434 (1970).
10. F.J. Zerilli and R.W. Armstrong, *J. Appl. Phys.* 61, 1816 (1987).
11. F.J. Zerilli, *Metall. Mater. Trans. A* 35A, 2547 (2004).
12. R.W. Armstrong, *Canad. Metall. Q.* 13, 187 (1974).
13. C. Zener and J.H. Hollomon, *J. Appl. Phys.* 15, 22 (1944).
14. F.J. Zerilli, R.W. Armstrong, in *Shock Compression of Condensed Matter—1995*, ed. S.C. Schmidt, W.C. Tao (American Institute of Physics, Woodbury, 1996), CP370, Part 1, p. 315.
15. J. Weertman, Chapter 13.*Mechanics and Materials; Fundamentals and Linkages*, ed. M.A. Meyers, R.W. Armstrong, and H.O.K. Kirchner (New York: Wiley Interscience, 1999), p. 451.
16. M.A. Przystupa and A.J. Ardell, *Metall. Mater. Trans. A* 33A, 231 (2002).
17. A.J. Ardell and M.A. Przystupa, *Mech. Mater.* 3, 319 (1984).
18. R.W. Armstrong, H. Conrad, and F.R.N. Nabarro, *Mechanical Properties of Nanostructured Materials and Nanocomposites*, ed. I. Ovid'ko, C.S. Pande, R. Krishnamoorti, E. Lavernia, and G. Skandan (Warrendale: Material Research Society, 2004), p. 69.
19. T.G. Langdon, *J. Mater. Sci.* 41, 597 (2006).
20. W. Blum and X.H. Zeng, *Acta Mater.* 57, 1966 (2009).
21. W. Blum, Y.J. Li, Y. Zhang, and J.T. Wang, *Mater. Sci. Eng. A* 528, 8621 (2011).
22. W. Blum, J. Dvořák, P. Král, P. Eisenlohr, and V. Sklenička, *Mater. Sci. Eng. A* 590, 423 (2014).
23. W. Blum, J. Dvořák, P. Král, M. Petranec, P. Eisenlohr, and V. Sklenička, *Philos. Mag.* 95, 3696 (2015).
24. J.H. Schneibel, M. Heilmaier, W. Blum, G. Hasemann, and T. Shanmugasundaram, *Acta Mater.* 59, 1300 (2011).
25. S.D. Antolovich and R.W. Armstrong, *Prog. Mater. Sci.* 59, 1 (2014).
26. R.W. Armstrong, J.H. Bechtold, R.T. Begley, in *Refractory Metals and Alloys II, TMS-AIME Metallurgical Society Conferences, 17*, ed. by M. Semchyshen, I. Perlmutter (Interscience Publishers, New York, 1963), p. 159.
27. Y.J. Li, J. Mueller, H.W. Höppel, M. Göken, and W. Blum, *Acta Mater.* 55, 5708 (2007).
28. Q. Wei and L.J. Kecskes, Chapter 8.*Mechanical Properties of Nanocrystalline Materials*, ed. J.C.M. Li (Singapore: Pan Stanford Publishers, Ltd., 2011), p. 213.
29. L. Lu and K. Lu, Chapter 6.*Mechanical Properties of Nanocrystalline Materials*, ed. J.C.M. Li (New York: Pan Stanford Publishers Ltd, 2011), p. 163.
30. N. Balasubramanian and T.G. Langdon, *Metall. Mater. Trans. A* 47A, 5827 (2016).
31. M. Kawasaki and T.G. Langdon, *J. Mater. Sci.* 51, 19 (2016).
32. M. Kawasaki, N. Balasubramanian, and T.G. Langdon, *Mater. Sci. Eng. A* 528, 6624 (2011).
33. A.K. Mukherjee, *Mater. Sci. Eng. A* 322, 1 (2002).
34. K.A. Padmanabhan, J. Leuthold, G. Wilde, and S.S. Bhattacharya, *Mech. Mater.* 91, 177 (2015).
35. H. Conrad: *J. Inst. Met.*, 87, 347 (1958–59).
36. U.F. Kocks and H. Mecking, *Prog. Mater. Sci.* 48, 171 (2003).
37. F.J. Zerilli and R.W. Armstrong, *J. Appl. Phys.* 68, 1580 (1990).
38. G.R. Johnson, W.H. Cook, *Proceedings of the 7th International Symposium on Ballistics* (The Hague, TN, 1983), p. 541.
39. H. Zhan, G. Wang, D. Kent, and M. Dargusch, *Mater. Sci. Eng. A* 612, 71 (2014).
40. T. Mirzaie, H. Mirzadeh, and J.-M. Cabrera, *Mech. Mater.* 94, 38 (2016).
41. A.H. Ammouri, G. Kridli, G. Ayoub, and R.F. Hamade, *J. Mater. Process. Technol.* 222, 301 (2015).
42. R.W. Armstrong: in *Nanometals—Status and Perspective, 33rd Risoe International Symposium on Materials Science*, ed. by S. Faester, N. Hansen, X. Huang, D. Juul Jensen, B. Ralph (Technical University of Denmark, Roskilde, 2012), p. 181.

43. A.H. Ammouri and R.F. Hamade, *Mater. Des.* 57, 673 (2014).
44. C.J. Chang, C.J. Lee, and J.C. Huang, *Scr. Mater.* 51, 509 (2004).
45. F.R. Larson and J. Miller, *Trans. ASME* 74, 765 (1952).
46. M. Tamura, F. Abe, K. Shiba, H. Sakasegawa, and H. Tanigawa, *Metall. Mater. Trans. A* 44A, 2645 (2013).
47. F. Abe, *Metall. Mater. Trans. A* 46A, 5610 (2015).